

Comparisons Between Histology and Optical Coherence Tomography Angiography of the Periarterial Capillary-Free Zone



CHANDRAKUMAR BALARATNASINGAM, DONG AN, YOICHI SAKURADA, CECILIA S. LEE, AARON Y. LEE, IAN L. MCALLISTER, K. BAILEY FREUND, MARINKO SARUNIC, AND DAO-YI YU

• **PURPOSE:** To use the capillary-free zone along retinal arteries, a physiologic area of superficial avascularization, as an anatomic paradigm to investigate the reliability of optical coherence tomography angiography (OCTA) for visualizing the deep retinal circulation.

• **DESIGN:** Validity analysis and laboratory investigation.

• **METHODS:** Five normal human donor eyes (mean age 69.8 years) were perfusion-labeled with endothelial antibodies and the capillary networks of the perifovea were visualized using confocal scanning laser microscopy. Regions of the capillary-free zone along the retinal artery were imaged using OCTA in 16 normal subjects (age range 24–51 years). Then, 3 × 3-mm scans were acquired using the RTVue XR Avanti (ver. 2016.1.0.26; Optovue, Inc, Fremont, California, USA), PLEX Elite 9000 (ver. 1.5.0.15909; Zeiss Meditec, Inc, Dublin, California, USA), Heidelberg Spectralis OCT2 (Family acquisition module 6.7.21.0; Heidelberg Engineering, Heidelberg, Germany), and DRI-OCT Triton (Ver. 1.1.1; Topcon Corp, Tokyo, Japan). Images of the superficial plexus, deep vascular plexus, and a slab containing all vascular plexuses were generated using manufacturer-recommended default settings. Comparisons between histology and OCTA were performed.

• **RESULTS:** Histologic analysis revealed that the capillary-free zone along the retinal artery was confined to the plane of the superficial capillary plexus and did not include the intermediate and deep capillary plexuses. Images derived from OCTA instruments demonstrated a

prominent capillary-free zone along the retinal artery in slabs of the superficial plexus, deep plexus, and all capillary plexuses. The number of deep retinal capillaries seen in the capillary-free zone was significantly greater on histology than on OCTA ($P < .001$).

• **CONCLUSION:** Using the capillary-free zone as an anatomic paradigm, we show that the deep vascular beds of the retina are not completely visualized using OCTA. This may be a limitation of current OCTA techniques. (Am J Ophthalmol 2018;189:55–64. © 2018 Elsevier Inc. All rights reserved.)

OPTICAL COHERENCE TOMOGRAPHY ANGIOGRAPHY (OCTA) is a relatively new imaging technique that is being rapidly incorporated into the management paradigms of retinal vascular diseases.^{1,2} Major advantages of OCTA include short image acquisition times and the ability to depth-resolve retinal vascular networks without the administration of dye. Aside from OCTA, there is a relative lack of in vivo imaging devices that allow reproducible visualization of vascular structures at the capillary level (where neurovascular coupling and nutrient/waste exchange occurs).³ Therefore, OCTA could potentially enhance our understanding of retinal vascular physiology and disease. Similar to OCTA, adaptive optics scanning laser microscopy⁴ is capable of providing exquisite visualization of retinal capillary structures, but technological barriers currently preclude its widespread use in clinical practice.

Few studies have compared the retinal vascular information seen on OCTA against the histologic gold standard.^{5,6} Consequently, it is unclear if OCTA allows complete visualization of all capillary structures within a vascular bed, especially those within the deeper layers of the retina. The capillary-free zone along retinal arteries is an area of physiologic avascularization that forms during embryogenesis. Histologic studies have shown that the capillary-free zone is confined to the plane of the superficial capillary plexus and does not involve the deeper capillary beds in the human perifovea.⁷ For this reason, the capillary-free zone provides a unique anatomic model for investigating the capabilities of OCTA for visualizing the deep retinal circulation. This report is a focused evaluation of the human perifoveal capillary-free zone using 4 different

Accepted for publication Feb 11, 2018.

From the Centre for Ophthalmology and Visual Science, University of Western Australia, Perth, Australia (C.B., D.A., I.L.M., D.-Y.Y.); Lions Eye Institute, Nedlands, Australia (C.B., D.A., I.L.M., D.-Y.Y.); Department of Ophthalmology, Sir Charles Gairdner Hospital, Nedlands, Australia (C.B.); LuEsther T. Mertz Retinal Research Center, Manhattan Eye, Ear and Throat Hospital, New York, New York (Y.S., K.B.F.); Department of Ophthalmology, University of Yamanashi, Yamanashi, Japan (Y.S.); Department of Ophthalmology, University of Washington, Seattle, Washington (C.S.L., A.Y.L.); Department of Ophthalmology, Royal Perth Hospital, Perth, Australia (I.L.M.); Vitreous, Retina, Macula Consultants of New York, New York (K.B.F.); Department of Ophthalmology, New York University School of Medicine, New York, New York (K.B.F.); and School of Engineering Science, Simon Fraser University, Burnaby, Canada (M.S.).

Inquiries to Dao-Yi Yu, Centre for Ophthalmology and Visual Science, Lions Eye Institute, University of Western Australia, 2 Verdun St, Perth, Australia; e-mail: dyyu@lei.org.au

OCTA instruments. Comparisons between OCTA and perfusion-labeled human donor histology are performed. The results of this study highlight some of the current limitations of OCTA.

METHODS

THIS STUDY IS A VALIDITY ANALYSIS AND LABORATORY investigation that followed the tenets of the Declaration of Helsinki. The study was approved by the Institutional Review Board at North Shore Long Island Jewish Health System and the Human Research Ethics Committee at the University of Western Australia. Written consent was obtained from all subjects.

• **HISTOLOGY AND CONFOCAL SCANNING LASER MICROSCOPY:** Five human eyes from 3 donors (1 male and 2 female) were obtained from DonateLife WA, the organ and tissue retrieval authority in Western Australia. The age of the human donors was 69.8 ± 10.5 years. Causes of death included cardiac arrest, lymphoma, and glioblastoma. Mean time from death to enucleation was 3.8 ± 0.8 hours. None of the donors had a history of eye disease.

Enucleated donor eyes underwent vascular endothelial labeling using our previously reported perfusion techniques. Detailed information regarding this methodology can be found in prior publications.^{8,9} In brief, the central retinal artery was cannulated using a glass micropipette (100 μ m tip diameter). The cannulated eye was initially perfused with 1% bovine serum albumin dissolved in Ringer's lactate solution to wash out residual blood clots. Eyes were subsequently perfused with 0.02 mg lectin-fluorescein isothiocyanate (FITC, Sigma-Aldrich Product No. L4895; Sigma-Aldrich, Darmstadt, Germany) mixed with 1 mL of 0.1% phosphate buffer to achieve endothelial labeling. The perfusate also contained 1 μ g Hoechst (Sigma-Aldrich Product No. H6024; Sigma-Aldrich, Darmstadt, Germany) for nuclear labeling. Retinas were subsequently dissected, flat-mounted on glass slides, and evaluated using confocal scanning laser microscopy (Nikon Eclipse 90i, Nikon Corporation, Tokyo, Japan) using 4 \times , 10 \times , and 40 \times objective lenses. Confocal stacks, of 2- μ m step sizes, extending from the inner limiting membrane to the outer nuclear layer were captured. Nuclei and vasculature were visualized using 408 nm/488 nm argon laser excitation with emissions detected through 450 nm/515 nm band-pass filters, respectively. Microscopic analysis was confined to the perifoveal region of the retina as defined by Hogan and associates.¹⁰ Specifically, images were acquired within an annulus that was 1.5 mm wide and an outer boundary located 2.75 mm from the foveal center. The capillary-free zone adjacent to the retinal arteries in the perifovea was captured in all images. This region will henceforth be referred to as the "capillary-free

zone." Confocal stacks of regions of interest were stratified into superficial capillary plexus (located within the nerve fiber layer and retinal ganglion cell layer), intermediate capillary plexus (located within the deep portion of the inner plexiform layer and superficial portion of the inner nuclear layer), and deep capillary plexus (located within the deep portion of the inner nuclear layer and the outer plexiform layer), as defined by previous reports.^{11,12} Nuclear labeling was used to judge the depth of capillary beds along the z-axis and to co-localize capillary beds to different retinal layers. Confocal image files were processed with IMARIS (Bitplane, Zurich, Switzerland) and/or ImageJ (Rasband, WS, ImageJ, U. S. National Institutes of Health, Bethesda, Maryland, USA; <https://imagej.nih.gov/ij/>) to create 2- and 3-dimensional projections of capillary beds.

• **OPTICAL COHERENCE TOMOGRAPHY ANGIOGRAPHY:** A total of 32 perifoveal locations were imaged from 16 normal human subjects using OCTA. Most subjects were imaged with only 1 device and some were imaged with 2 devices. Demographic details of subjects are summarized in the Table. All subjects had a visual acuity of 20/20 or better. None of the subjects had a history of eye disease.

Commercial OCTA devices used for patient imaging including the RTVue XR Avanti (ver. 2016.1.0.26; Optovue, Inc, Fremont, California, USA), PLEX Elite 9000 (ver. 1.5.0.15909; Zeiss Meditec, Inc, Dublin, California, USA), Heidelberg Spectralis OCT2 (Family acquisition module 6.7.21.0; Heidelberg Engineering, Heidelberg, Germany), and DRI-OCT Triton (Ver. 1.1.1; Topcon Corp, Tokyo, Japan). Software and hardware specifications for these devices are summarized in the Table. All OCTA devices acquired a 3 mm \times 3 mm volume scan. Images of the superficial capillary plexus, deep vascular plexus, and a slab containing all vascular plexuses was generated using manufacturer-recommended default settings. Similar to histology, images were acquired from the perifovea and included the capillary-free zone. OCTA images were evaluated by 2 of the authors (C.B. and D.A.) and regions were re-scanned or excluded if original images were of poor quality or contained artefacts that precluded reliable image analysis. The signal strength ranges for images from each of the OCTA devices were as follows: Optovue, signal strength 62-72; Heidelberg, Q-score 32-40; Zeiss, signal strength 8; and Triton, image quality 63-73.

• **COMPARISONS BETWEEN OPTICAL COHERENCE TOMOGRAPHY ANGIOGRAPHY AND HISTOLOGY:** Morphologic patterns and locations of capillary structures as seen on OCTA and histology were compared. OCTA and histology images were cropped such that the area of the region of interest was identical. A total of 16 OCTA images (RTVue XR Avanti = 3, Heidelberg OCT2 = 3, PLEX Elite 9000 = 6, and DRI OCT Triton = 4) and 11 histology images acquired from 5 donor eyes were quantitatively analyzed using ImageJ (version 1.43; National

TABLE. Demographic Details and Specifications of Optical Coherence Tomography Angiography Devices

OCTA Device	Wavelength (nm)	A-scan Rate (kHz)	Algorithm	Motion Artefact Minimization	Total Subjects	Male	Age Range (Years)	Total Regions Imaged
RTVue XR	840	70	SSADA	Orthogonal registration	5	3	24–51	10
Heidelberg OCT2	870	85	FS-ADA	Eye tracking (Truetrack)	5	3	24–51	10
PLEX Elite 9000	1040–1060	100	OMAG	Eye tracking (FastTrac)	3	1	27–34	6
DRI OCT Triton	1050	100	OCTARA	Eye tracking (SMARTTrack)	3	1	27–34	6

FS-ADA = full-spectrum amplitude decorrelation algorithm; OCTA = optical coherence tomography angiography; OCTARA = OCTA ratio analysis; OMAG = optical microangiography; SSADA = split-spectrum amplitude decorrelation angiography.

Institutes of Health, Bethesda, Maryland, USA; <http://rsb.info.nih.gov/ij/>). OCTA slabs that depicted all vascular layers in the retina (segmentation boundaries spanning across the entire retinal thickness) were used for quantitative analysis. Accordingly, histologic images that were used for analysis also comprised all capillary networks in the retina projected into a single image. The number of capillaries visualized in the capillary-free zone, per 100 μm of retinal artery length, was determined through manual counting.

RESULTS

• **HISTOLOGIC CHARACTERISTICS OF THE PERIFOVEAL CIRCULATION:** The histologic characteristics of capillary networks that comprise the human perifoveal circulation are illustrated in [Figure 1](#). Projection of all capillary networks into a single 2-dimensional image revealed a dense network of vascular structures per area of tissue. Stratified evaluation of the circulation into individual capillary beds demonstrated that the superficial capillary plexus was localized within the nerve fiber layer and retinal ganglion cell layer. Radial peripapillary capillaries, characterized by relatively long and straight capillary segments with shorter intercapillary connections, were seen in the perifoveal regions close to the optic disc.

The intermediate capillary plexus was significantly more 3-dimensional in configuration than other networks in the perifovea. This plexus was characterized by irregular vascular loops and vertical capillary segments that adjoined the superficial and deep capillary networks.

The deep capillary plexus was significantly planar and 2-dimensional in its configuration. A high number of closed capillary loops were seen within the deep plexus.

Projection of all confocal slices that comprised the intermediate plexus into a 2-dimensional image resulted in oblique and incomplete vascular loops that could be clearly distinguished when viewed in 3 dimensions, assuming a planar closed-loop configuration that appeared similar to the deep capillary plexus ([Figure 2](#)). The morphologic differences between the intermediate and deep capillary plexuses were more apparent when these networks were visualized in 3 dimensions ([Figure 2](#)).

Retinal arteries and veins were predominantly confined to the plane of the superficial capillary plexus; however, the undulating nature of retinal arteries and veins resulted in portions of these structures abutting the plane of the intermediate plexus. None of the histologic specimens demonstrated segments of retinal arteries or veins at the level of the deep capillary plexus. Retinal arteries in the perifovea were characterized by a capillary-free zone (approximately 30–50 μm in diameter) on either side of the vascular lumen ([Figure 1](#)). Prominent capillary-free zones were not associated with retinal veins. Three-dimensional and cross-sectional analysis of capillary-free zones revealed that they were only confined to the plane of the superficial plexus. Vascular structures arising from the intermediate and deep capillary plexus were clearly seen to bridge beneath the retinal artery in all cases ([Figure 1](#)), demonstrating that the capillary-free zone only involved the superficial plexus.

• **COMPARISONS BETWEEN OPTICAL COHERENCE TOMOGRAPHY ANGIOGRAPHY AND HISTOLOGY:** Images of the superficial capillary bed, deep capillary bed, and a slab comprising all capillary beds using manufacturer-recommended default settings from the 4 OCTA devices are provided in [Figures 3, 4, and 5](#), respectively. The same eyes are presented across these figures. Representative histologic images are also provided for comparisons in each of these figures.

In all OCTA devices, the retinal arteries and veins were seen in the slab representing the superficial capillary bed ([Figure 3](#)). Long and straight capillary segments that resembled the radial peripapillary capillaries were evident in slabs acquired near the optic disc. A capillary-free zone, devoid of vascular structures, was evident adjacent to retinal arteries in all devices ([Figure 3](#), insets).

The retinal artery and vein were seen in many OCTA slabs depicting the deep capillary bed ([Figure 4](#)). A prominent capillary-free zone, resembling that seen in the superficial capillary bed, was visible on OCTA images of the deep capillary bed represented in the PLEX Elite 9000, Heidelberg OCT2, and RTVue XR Avanti ([Figure 4](#), insets).

All devices demonstrated a prominent capillary-free zone on slabs depicting all capillary beds within the retina

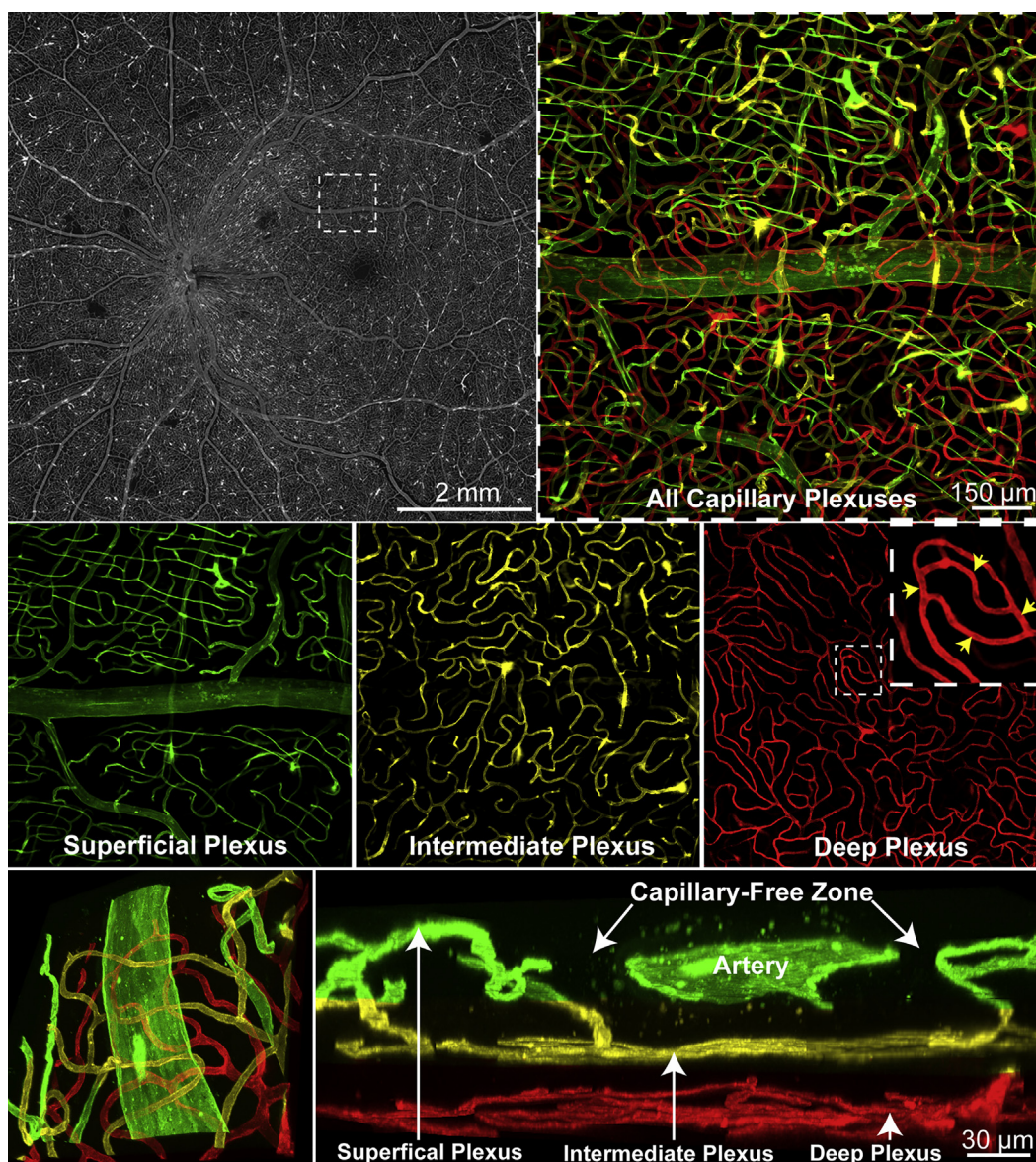


FIGURE 1. Histologic characteristics of the human perifoveal circulation. Wide-field confocal microscope image of a perfusion-labeled human donor specimen (Top left) demonstrates complete vascular labelling. Magnified view of inset, which includes a major retinal artery, is shown at Top right. A color-coded 2-dimensional projection of all vascular structures within the region of interest is provided. Note the high density of vascular structures within the perifovea. Stratification of the confocal stack into different capillary beds demonstrates the varying morphologies of the superficial plexus, intermediate plexus, and deep plexus (Middle row). The deep plexus is characterized by numerous vascular loops (Middle right, inset) with closed boundaries (yellow arrows). Magnified 3-dimensional (Bottom left) and cross-sectional (Bottom right) views of a major perifoveal artery demonstrate a capillary-free zone immediately adjacent to the lumen at the level of the superficial plexus. Capillaries of the intermediate and deep plexus are seen to clearly bridge under the retinal arteries. In all panels, the superficial plexus has been false-colored green, the intermediate plexus false-colored yellow, and the deep plexus false-colored red.

(Figure 5). This included the DRI OCT Triton, where a prominent capillary-free zone was not evident in slabs of the deep capillary bed. The number of capillaries per 100 µm of retinal artery in the capillary-free zone was significantly greater on histology images (1.80 ± 0.33) than in OCTA (0.60 ± 0.19 ; $P < .001$).

DISCUSSION

THIS REPORT COMPARED THE TOPOGRAPHIC CHARACTERISTICS of the capillary-free zone between OCTA and human donor histology. The perifovea was chosen as the region of interest for several reasons: (1) the histologic

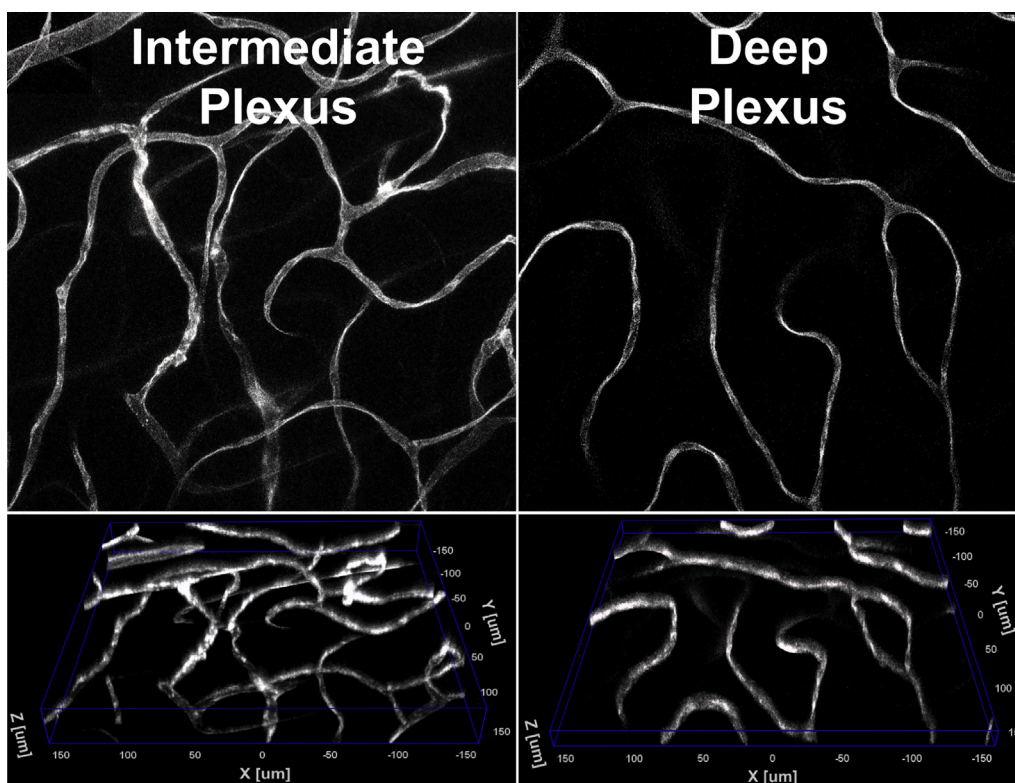


FIGURE 2. Histologic comparisons between the intermediate and deep plexus as seen in 2 and 3 dimensions. Although the intermediate plexus is largely a 3-dimensional network with oblique and irregular loops, projection of this plexus into a 2-dimensional image (Top left) creates the impression that it is also composed of many closed loops like the deep plexus (Top right) owing to overlapping of capillary segments along the z-axis. Visualization of the same networks in 3 dimensions (Bottom left: intermediate plexus; Bottom right: deep plexus) clearly demonstrates the morphologic distinctions, namely that the deep plexus is a predominantly planar and 2-dimensional network. Images in the lower panels have been represented with an identical degree of tilt.

characteristics of the perifoveal circulation is well defined,^{11,12} (2) the perifovea has been studied in less detail using OCTA than the central macula, and (3) the total thickness of the perifovea is comparable to the central macula¹⁰ but the absence of the foveal clivus makes it less susceptible to automated OCTA segmentation errors.

Recently, Spaide and Curcio compared the appearance of the superficial and deep capillary plexus in a single eye using 3 different OCTA instruments.¹³ They compared the manufacturer-stated segmentation boundaries for each instrument against a single histologic cross section and demonstrated that portions of the deep vascular plexus were represented in the superficial slab of the central macula. Munk and associates¹⁴ acquired contemporaneous OCTA images of the central macula from 19 normal subjects using 4 OCTA instruments and demonstrated significant inter-instrument differences in density measurements of the superficial capillary plexus. They proposed that variations in manufacturer-stated segmentation boundaries may be one reason for these differences. Recent work has identified inter-instrument inconsistencies in the boundaries used to define the deep capillary beds of the

retina.^{15,16} Some instruments segment the deep vascular complex (composed of the intermediate and deep capillary plexuses), while others segment the deep capillary plexus in isolation. The main purpose of our study was not to investigate inter-instrument variations in segmentation boundaries; however, we found that retinal arteries and veins were represented in some OCTA images of the deep capillary plexus. When histologic examination was performed, it was evident that the outer boundaries of the retinal arteries and veins did not extend to the level of the deep capillary plexus. One reason why retinal arteries and veins were seen in the deep plexus may have been because of projection artefact.¹⁷

The capillary-free zone along the retinal artery is a useful experimental model for studying the anatomic characteristics of the deep retinal circulation, as it is inherently devoid of the superficial capillary plexus. Michaelson and Campbell⁷ were among the earliest investigators to histologically demonstrate the presence of a capillary-free zone along human retinal arteries. As transmural oxygen diffusion is capable of satisfying the metabolic demands of cells immediately adjacent to the retinal artery, a capillary-free zone develops during embryogenesis.⁷ However, oxygen

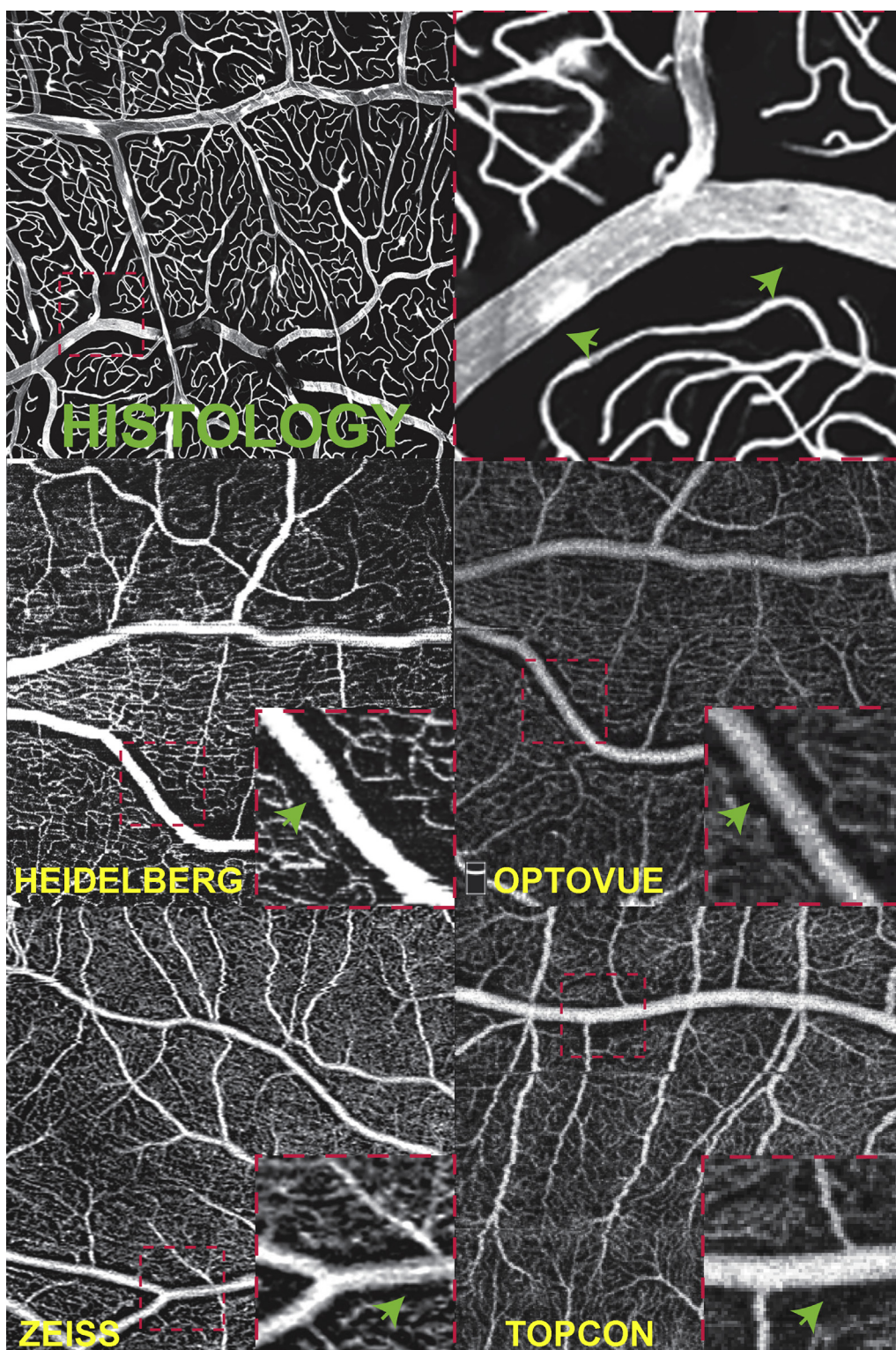


FIGURE 3. Optical coherence tomography angiography (OCTA) of the superficial plexus. The histologic characteristics of the superficial plexus are shown in the Top left panel. Magnified view of inset is shown in the Top right panel, where the periarterial capillary-free zone is clearly evident. Representative scans of the superficial plexus using the Heidelberg Spectralis OCT2 (Middle left), Angiovue Optovue RTVue XR Avanti (Middle right), PLEX Elite 9000 (Bottom left), and DRI OCT Triton (Bottom right) are provided. Note that retinal arteries and veins are seen in the plane of the superficial capillary plexus in OCTA and histologic images. A prominent capillary-free zone is evident adjacent to retinal arteries (green arrows).

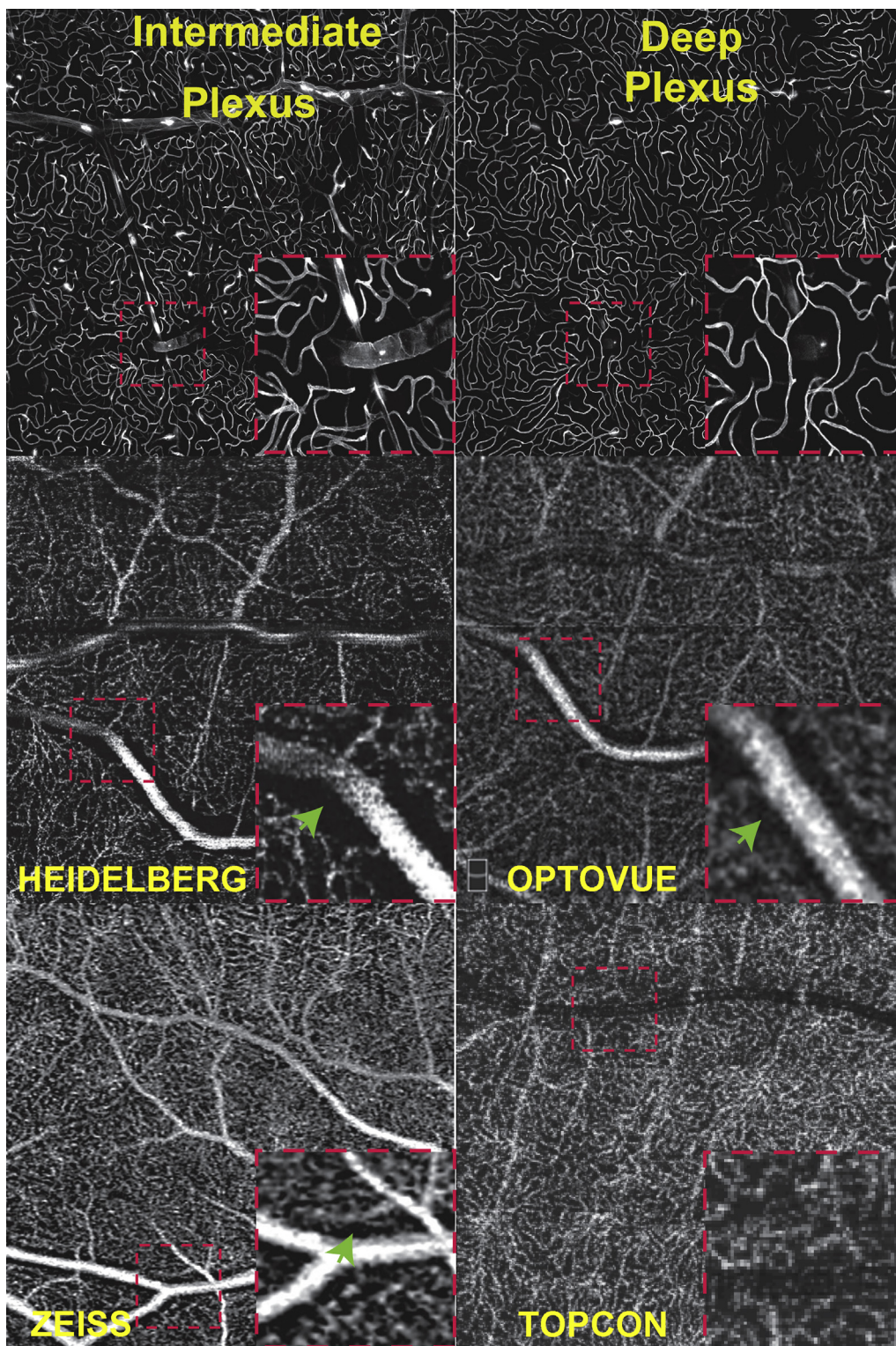


FIGURE 4. Optical coherence tomography angiography (OCTA) of the deep plexus. The histologic characteristics of the intermediate plexus and deep plexus of the same eye from the same region of interest are shown in the Top left and Top right panels, respectively. A segment of the retinal artery is seen in the histologic image of the intermediate plexus (Top left inset) but not the deep plexus (Top right inset). Representative scans of the deep plexus using the Heidelberg Spectralis OCT2 (Middle left), Angiovue Optovue RTVue XR Avanti (Middle right), PLEX Elite 9000 (Bottom left), and DRI OCT Triton (Bottom right) are provided. Note that the entire length of the retinal artery and vein are visualized in the deep plexus of some instruments. Magnified views of the retinal artery (insets, Middle and Lower panels) demonstrate a prominent capillary-free zone in 3 of the OCTA images (green arrows). Note that such a capillary-free zone is not evident adjacent to retinal veins.

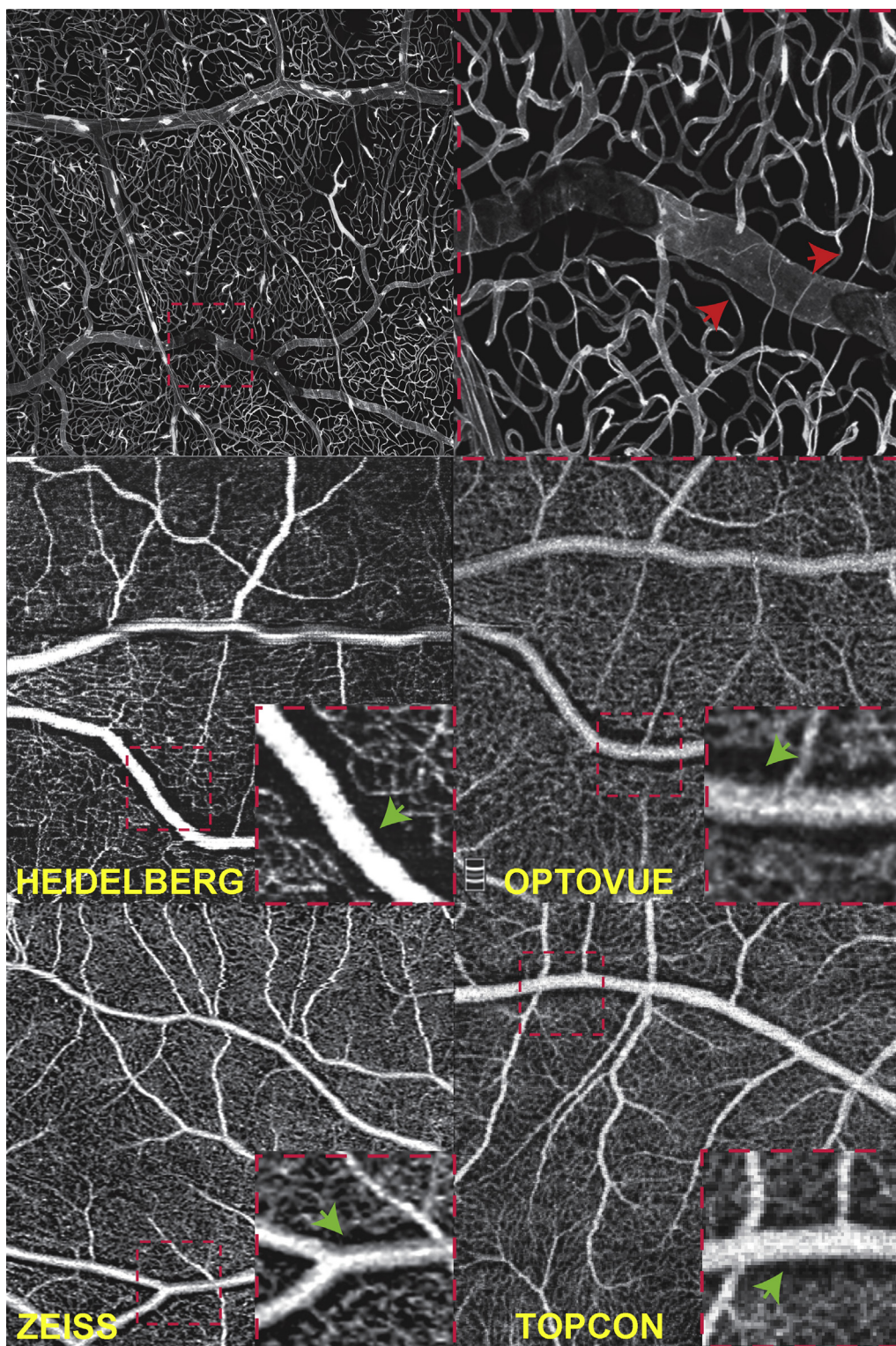


FIGURE 5. Optical coherence tomography angiography (OCTA) of all capillary plexuses. Histologic appearance of all retinal capillary plexuses projected as a single image is presented in the Top left panel. Magnified view of the retinal artery is shown in the Top right panel. Note that the capillary-free zone is not histologically evident when all the plexuses are projected into a single image, as numerous capillaries (red arrows) are seen to pass under the artery and bridge the periarterial capillary-free zone. Representative scans of all capillary plexuses using the Heidelberg Spectralis OCT2 (Middle left), Angiovue Optovue RTVue XR Avanti (Middle right), PLEX Elite 9000 (Bottom left), and DRI OCT Triton (Bottom right) are provided. Closer view of the retinal artery (insets, Middle and Lower panels) using OCTA demonstrates a prominent capillary-free zone on all instruments.

diffusion occurs across a finite distance and oxygen tension within the retinal veins is low.¹⁸ Therefore, capillary-free zones do not traverse the entire thickness of the retina and are not prominent around retinal veins. Histologic evaluation of donor specimens in our study reaffirmed that the capillary-free zone was confined to the plane of the superficial plexus in the perifovea and did not involve other capillary networks. Numerous capillary segments arising from the intermediate and deep capillary plexus were seen beyond the outer boundaries of the capillary-free zone on histologic specimens. In comparison, OCTA images of the superficial capillary bed, deep capillary bed, and all capillary beds were largely devoid of flow signals within the capillary-free zone, creating the impression that the capillary-free zone involved all capillary plexuses. As the appearance of the capillary-free zone was not significantly different between slabs representing the deep capillary bed (Figure 4) and those involving all capillary beds (Figure 5) in 3 out of 4 devices, it is unlikely that segmentation error or artefact accounted for this appearance. Interestingly, the capillary-free zone was not clearly seen in slabs of the deep capillary beds on the DRI OCT Triton but appeared quite prominent in slabs depicting all vascular beds.

The deep capillary plexus is arguably the vascular bed that is most vulnerable to injury. For example, microaneurysms are one of the earliest vascular changes that characterize diabetic retinopathy and are most commonly found in the deep layers of the retina.¹⁹ Techniques that permit precise in vivo visualization of the deep circulation may therefore play a vital role in early disease detection. As shown in this study, a possible limitation of OCTA is that it may provide incomplete information of the deep retinal vascular beds and may therefore not be able to detect the earliest markers of retinal vascular disease. Previous studies have shown that OCTA-derived measurements of capillary

density and foveal avascular zone morphology correlate with the degree of vision loss in diabetic retinopathy and retinal vein occlusion.^{20,21} Our study does not refute these previous findings but serves to highlight areas where the technique of OCTA can be improved. One possible reason why capillary structures comprising the deeper capillary beds are not clearly visualized using OCTA may be owing to reduced flow rates within these vascular beds relative to the superficial circulation. As such, flow rates in the deep circulation may frequently fall below the threshold required to register an OCTA flow signal. Oxygen consumption is not homogeneous across the retina,²² and it is plausible that slower flow rates are required in the deeper circulations to optimize nutrient/waste exchange between neurons and capillaries. We emphasize that this is a speculation and such a hypothesis was not specifically investigated in this study.

In this study we also show that the morphologic characteristics of the intermediate capillary plexus and deep capillary plexus are similar when volumetric data from each of these capillary beds are projected into a single image and examined in 2 dimensions. For this reason, when OCTA data are not evaluated in 3 dimensions, it may not be possible to reliably distinguish disease processes that arise from the intermediate and deep capillary plexuses. This may in turn result in imprecise attribution of the origin of disease processes within the retina.

We acknowledge several limitations of this study; namely, that imaging data were analyzed in a qualitative fashion and that histology and OCTA data were acquired from separate cohorts. Additionally, we only analyzed 4 OCTA instruments from a cohort of limited sample size. A major strength of this study is that perfusion-labeled histology and confocal scanning laser microscopy was used to define OCTA histology correlates. To date, few studies have validated OCTA using such techniques.

FUNDING/SUPPORT: NATIONAL HEALTH AND MEDICAL RESEARCH COUNCIL OF AUSTRALIA; LUESTHER T. MERTZ RETINAL Research Center, Manhattan Eye, Ear and Throat Hospital, New York, New York, USA; The Macula Foundation, Inc, New York, New York, USA. The study used the Zeiss Plex Elite 9000 to collect data from subjects, from the University of Washington and Vitreous, Retina, Macula Consultants of New York. At the University of Washington, the Zeiss Plex Elite 9000 is loaned equipment under an agreement between University of Washington and Carl Zeiss Meditec Inc. Financial Disclosures: Chandrakumar Balaratnasingam is a consultant to Novartis, Allergan and Bayer (honorarium for each). IL McAllister is a consultant to Novartis and Bayer. Aaron Y. Lee has research funding from Novartis, NVIDIA Corporation, and Microsoft Corporation. K. Bailey Freund is a consultant to Genentech, Optos, Optovue, GrayBug Vision, and Heidelberg Engineering (honorarium from each) and receives research support from Genentech/Roche. The following authors have no financial disclosures: Dong An, Yoichi Sakurada, Cecilia S. Lee, Ian L. McAllister, Marinko Sarunic, and Dao-Yi Yu. The authors attest that they meet the current ICMJE criteria for authorship.

REFERENCES

1. Lee J, Rosen R. Optical coherence tomography angiography in diabetes. *Curr Diab Rep* 2016;16(12):123.
2. Sambhav K, Grover S, Chalam KV. The application of optical coherence tomography angiography in retinal diseases. *Surv Ophthalmol* 2017;62(6):838–866.
3. Usui Y, Westenskow PD, Kurihara T, et al. Neurovascular crosstalk between interneurons and capillaries is required for vision. *J Clin Invest* 2015;125(6):2335–2346.
4. Mo S, Krawitz B, Efstathiadis E, et al. Imaging foveal microvasculature: optical coherence tomography angiography versus adaptive optics scanning light ophthalmoscope fluorescein angiography. *Invest Ophthalmol Vis Sci* 2016;57(9):OCT130–OCT140.
5. Chan G, Balaratnasingam C, Xu J, et al. In vivo optical imaging of human retinal capillary networks using speckle

- variance optical coherence tomography with quantitative clinico-histological correlation. *Microvasc Res* 2015;100:32–39.
6. Tan PE, Balaratnasingam C, Xu J, et al. Quantitative comparison of retinal capillary images derived by speckle variance optical coherence tomography with histology. *Invest Ophthalmol Vis Sci* 2015;56(6):3989–3996.
 7. Michaelson IC, Campbell ACP. The anatomy of the finer retinal vessels, and some observations on their significance in certain retinal diseases. *Trans Ophthalmol Soc UK* 1940;60:71–111.
 8. Yu PK, Balaratnasingam C, Morgan WH, Cringle SJ, McAllister IL, Yu DY. The structural relationship between the microvasculature, neurons, and glia in the human retina. *Invest Ophthalmol Vis Sci* 2010;51(1):447–458.
 9. Yu PK, Balaratnasingam C, Cringle SJ, McAllister IL, Provis J, Yu DY. Microstructure and network organization of the microvasculature in the human macula. *Invest Ophthalmol Vis Sci* 2010;51(12):6735–6743.
 10. Hogan MJ, Alvarado JA, Weddell JE. Histology of the Human Eye: An Atlas and Textbook. Philadelphia: W.B. Saunders Company; 1971.
 11. Chan G, Balaratnasingam C, Yu PK, et al. Quantitative morphometry of perifoveal capillary networks in the human retina. *Invest Ophthalmol Vis Sci* 2012;53(9):5502–5514.
 12. Snodderly DM, Weinhaus RS, Choi JC. Neural-vascular relationships in central retina of macaque monkeys (*Macaca fascicularis*). *J Neurosci* 1992;12(4):1169–1193.
 13. Spaide RF, Curcio CA. Evaluation of segmentation of the superficial and deep vascular layers of the retina by optical coherence tomography angiography instruments in normal eyes. *JAMA Ophthalmol* 2017;135(3):259–262.
 14. Munk MR, Giannakaki-Zimmermann H, Berger L, et al. OCT-angiography: a qualitative and quantitative comparison of 4 OCT-A devices. *PLoS One* 2017;12(5):e0177059.
 15. Campbell JP, Zhang M, Hwang TS, et al. Detailed vascular anatomy of the human retina by projection-resolved optical coherence tomography angiography. *Sci Rep* 2017;7:42201.
 16. Gattoussi S, Freund KB. Correlating structural and angiographic optical coherence tomography in the intermediate and deep retinal capillary plexuses. *Exp Eye Res* 2017;165:96–98.
 17. Spaide RF, Fujimoto JG, Waheed NK. Image artifacts in optical coherence tomography angiography. *Retina* 2015;35(11):2163–2180.
 18. McLeod D. Krogh cylinders in retinal development, panretinal hypoperfusion and diabetic retinopathy. *Acta Ophthalmol* 2010;88(8):817–835.
 19. Moore J, Bagley S, Ireland G, McLeod D, Boulton ME. Three dimensional analysis of microaneurysms in the human diabetic retina. *J Anat* 1999;194(Pt 1):89–100.
 20. Balaratnasingam C, Inoue M, Ahn S, et al. Visual acuity is correlated with the area of the foveal avascular zone in diabetic retinopathy and retinal vein occlusion. *Ophthalmology* 2016;123(11):2352–2367.
 21. Samara WA, Shahlaee A, Adam MK, et al. Quantification of diabetic macular ischemia using optical coherence tomography angiography and its relationship with visual acuity. *Ophthalmology* 2017;124(2):235–244.
 22. Yu D-Y, Cringle SJ. Oxygen distribution and consumption within the retina in vascularised and avascular retinas and in animal models of retinal disease. *Prog Retin Eye Res* 2001;20(2):175–208.